Int. J. Electrochem. Sci., 14 **(2019)** 10983 – 10999, doi: 10.20964/2019.12.75

International Journal of
ELECTROCHEMICAL
SCIENCE
www.electrochemsci.org

Electrochemical Investigation of Passive Film Properties on Low Alloy Steel Rebars in Cement Extract and Saturated $Ca(OH)_2$ Solutions

Shimin Li[1], *Wei Liu*[1,*], *Yueming Fan*[1], *Yutao Wang*[1], *Banthukul Wongpat* [1], *Baojun Dong*[1], *Yonggang Zhao*[1], *Zhentao Wang*[1], *Yanliang Zhou*[1], *Thee Chowwanonthapunya*[2], *Xiaogang Li* [1]

[1] Corrosion and Protection Center, Institute for Advanced Materials and Technology, University of Science and Technology Beijing, Beijing 100083, China
[2] Faculty of International Maritime Studies, Kasetsart University, SiRacha 20230, Thailand
[*]E-mail: weiliu@ustb.edu.cn

Received: 7 May 2019 / *Accepted:* 16 July 2019 / *Published:* 29 October 2019

In this paper, the differences in the passivation behaviours of low alloy steel rebars in saturated $Ca(OH)_2$ solution (SC) and cement extract solution (CE) were studied by Mott-Schottky, XPS and cyclic potentiodynamic polarisation (CPP) analyses. The results indicate that the formation rate of a passive film in SC is faster than that in CE at the initial stage of immersion. With the same passivation time, the passive film that formed in CE has a lower self-corrosive current density, a greater film resistance, a thicker film and better stability than the film formed in SC. The passive films formed in SC and CE have the same composition, and they both exhibit n-type semiconductor characteristics, but the passive films formed in CE have a lower donor carrier concentration and better compactness than those formed in SC. The unpassivated steel has a higher critical Cl^- concentration in SC. However, after the steel rebar is passivated for 7 days, the critical Cl^- concentration in CE is higher than that in SC. The critical Cl^- concentration of passivated steel rebars is 4 times higher than that of unpassivated steel rebars, which indicates that passive films can significantly improve the pitting corrosion resistance of steel rebars.

Keywords: Low alloy steel rebars, Mott-Schottky, Cyclic potentiodynamic polarisation, Passive film, Critical Cl^- concentration

1. INTRODUCTION

Low alloy steel rebars are widely used for bridges, seaports and undersea tunnels due to their excellent mechanical properties and corrosion resistance [1-3]. In the process of using reinforced concrete, the hydration of cement in concrete produces a variety of hydroxides that make the pH value of electrolytes in concrete pores range from 12.5 to 13.5 [4-6]. Steel rebars are exposed to a highly alkaline environment, passive films will formed rapidly [7-9]. The composition and electrochemical

characteristics of the passive film are not only relevant to the types of alloying elements but also influenced by the types of ions in concrete pore solutions.

To explore the passivation mechanism of steel bars in concrete, chemical reagents are usually used to configure synthetic solutions to simulate the concrete pore solution [10-12]. Sánchez et al. [13] used saturated $Ca(OH)_2$ + KOH solutions to study the growth mechanism of passivation films under two passivation conditions: natural passivation and constant potential passivation; the results showed that the composition of passivation films and the electrochemical behaviours are significantly different under the two conditions. Shi et al. [14] studied the critical Cl^- concentration of unpassivated and pre-passivated steel bars in $Ca(OH)_2$ + KOH + NaOH solution with different Cl^- concentrations, and the results indicated that a passivation film can enhance the critical Cl^- concentration of the steel rebars. At present, there is no formal standard solution that is used for steel passivation film studies in the laboratory, and pore solution in an actual concrete environment is more complex. The kinds and contents of ions contained in the indoor solution are quite different from the actual concrete pore solution, so the indoor solution cannot accurately simulate the passivation of steel bar in the concrete. The ionic components in the concrete pore solution include Ca^{2+}, K^+, Al^{3+} and SO_4^{2-} ions, which mainly come from the hydration of cement, so it is more realistic to use cement extract to represent pore solutions [15]. Jiang et al. [16] studied the threshold of pitting corrosion of carbon steel rebars in saturated $Ca(OH)_2$ and cement solutions with multiple Cl^- types. The results showed that the threshold of pitting corrosion of steel rebars in cement extracts was higher than that of the $Ca(OH)_2$ solution. Peng et al. [17] studied the passivation process of P110 immersed in $Ca(OH)_2$ and cement extract solutions. The results showed that the stability level of the passivation film formed in those solutions was slightly different.

Low alloy steel rebar as a new type of corrosion resistant steel bar, the composition and electrochemical characteristics of passivation films are affected by alloying elements, and the formation mechanism of passive film is also different in different simulated concrete pore solutions. Current research focuses on the passivation formation process of low alloy steel rebars in a single solution, and there are few studies on the differences in structure, components and electrochemical behaviours of passivation films of low alloy steel rebars in indoor simulated solutions and real concrete environments. Therefore, it is necessary to further explore the differences in passivation films formed by low alloy steel rebars in different pore solutions.

In this paper, cement extract is used to represent real concrete environments, and a saturated $Ca(OH)_2$ solution is used to represent the indoor simulated solution. The passivation behaviour of low alloy steel rebars immersed in SC and CE with different times is studied by electrochemical methods such as electrochemical impedance spectroscopy(EIS), M-S and CPP curves, and the components of passivated films are studied by XPS,the research results are beneficial to the research and development of new steel rebars.

2. EXPERIMENTAL

2.1 Materials

The low alloy steel rebar used in this experiment is obtained by adding a certain amount of alloy elements to the carbon steel bar HRB400E. Table 1 shows the chemical composition of steel rebars (in unit % by mass). The sample was machined into dimensions of 10×10×5 mm, welding copper wire on the surface of bar, and then the sample was placed in a PVC pipe and sealed with an epoxy resin. Before the test, the surface of the sample was polished with 600, 800, and 1200# SiC sandpaper, and then the surface of the sample was cleaned with ethanol and dried.

Table 1. Chemical composition of the tested steel bar (wt.%)

Elements	C	Si	Mn	P	S	Cu	Ni	Mo	Cr	Fe
Weight-%	0.18	0.57	1.01	0.01	0.002	0.30	0.20	0.15	1.60	Bal.

2.2 Exposure solutions

(1) Cement extract solution (CE). Cement was poured into deionised water (C:W=1:10), stirred for 24 hours with a magnetic stirrer, and allowed to stand for 6 hours; then, the supernatant was taken as the cement extract (pH=12.6±0.2). The type of cement is PO 42.5R, whose mineral components are CaO, 61.28%, Al_2O_3, 9.34%, Fe_2O, 3.10, MgO, 1.35%, SiO_2, 22.75% and SO_3, 0.99% [18].

(2) Saturated $Ca(OH)_2$ solution (SC). Excess $Ca(OH)_2$ was dissolved in deionised water and stirred for 24 hours with a magnetic stirrer; then, the supernatant was taken after 6 hours of static storage (pH=12.6±0.2). All electrolytes were prepared with analytical reagents and distilled water.

2.3 Electrochemical measurements

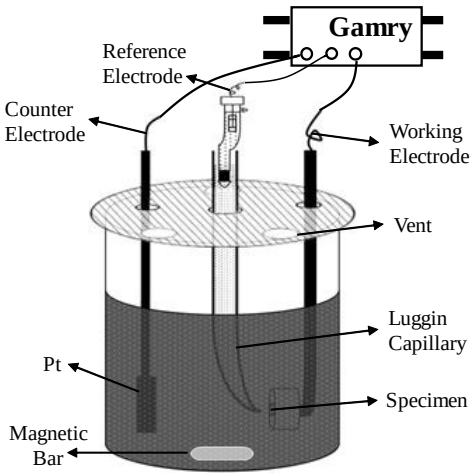

Figure 1. The illustration of three electrode system

The electrochemical properties of the samples were measured by using a Gamry electrochemical workstation. A steel sample was used as the working electrode, a saturated calomel electrode (SCE) was used as the reference electrode, and a platinum electrode was used as the counter electrode, as shown in Fig. 1.

The electrochemical characteristics of steel bar samples immersed for different times were measured. The EIS measurement frequency ranged from 10 KHz to 0.01 mHz, and a sinusoidal potential perturbation of 5 mV amplitude was applied. The measurement results were analysed by ZsimpWin software. The potential sweeping of polarisation curves was from -0.25 to 12 V (vs. OCP) at a scan rate of 0.1667 mV/s. Mott-Schottky experiments were performed on the passive film at a frequency of 1 kHz, with a step rate of 50 mV/s from −1.0 to +1.0 V_{SCE}.

Cyclic potentiodynamic polarisation (CPP) measurements were performed from a potential of -250 V_{OCP}, and the reverse polarisation scan was performed when the anode current density reached 200 μA/cm^2, with a scan rate of 1 mV/s. Before the CPP measurement, steel rebars without passivation and with passivation for 7 days were immersed for 48 hours in SC and CE with different Cl^- concentrations. The temperature of the solution was 30 ℃ to simulate a tropical marine atmosphere.

2.4 XPS

The composition of the passivation films on the steel bars was determined by XPS after the bars were immersed for 7 days in SC and CE.

3. RESULTS AND DISCUSSION

3.1 Open circuit potential

The slope of the OCP curve over time of the steel rebars in alkaline solution reflects the formation rate of passivation films [19]. Fig. 2 is the curve of the OCP with time in SC and CE. After an immersion time of 24 hours, the OCP in SC and CE has a positive shift of approximately 300 mV and then remains relatively stable. With a prolonged immersion time, the OCP values of the two curves show the same trend, and there are three stages (I, II, III) of the curves. Song et al. also found that the OCP curve of carbon steel rebars in SC over time has the same results [20]. In Part I, the OCP was rapidly shifted to the positive side, indicating that the formation rate in SC was fast. In this stage, the slope of curve 1 was larger than that of curve 2, which indicated that the formation rate of the passivation film in CE was slower than in SC. In the second stage, the slope of the curve was significantly reduced, and the rate of passivation film formation decelerated. This result is mainly due to the direct contact between the solution and the steel matrix at the beginning of the immersion, which is conducive to Fe dissolution; with the formation of a complete passive film on the steel matrix, the passive film will increase the resistance of the steel and cause the dissolution rate to decrease sharply [21]. In the third stage, the OCP of the two curves tends to be stable, and the OCP corresponding to the CE curve is higher, indicating that the corrosion tendency of the steel bar is lower in CE.

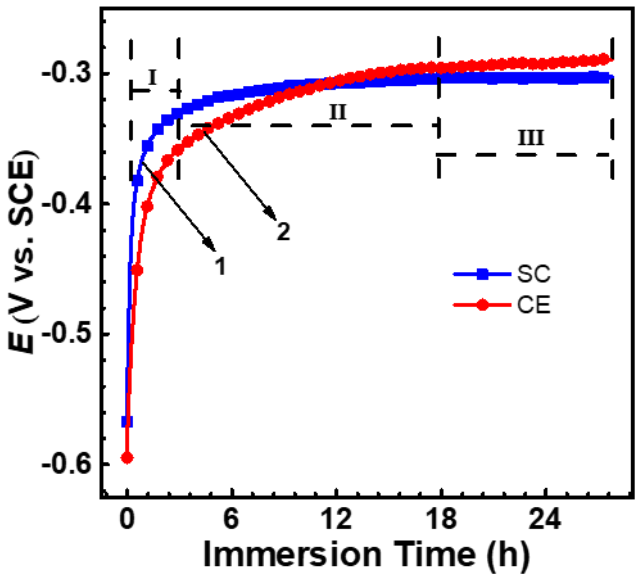

Figure 2. The curve of OCP over time the steel rebars in SC and CE

3.2 Polarisation curves

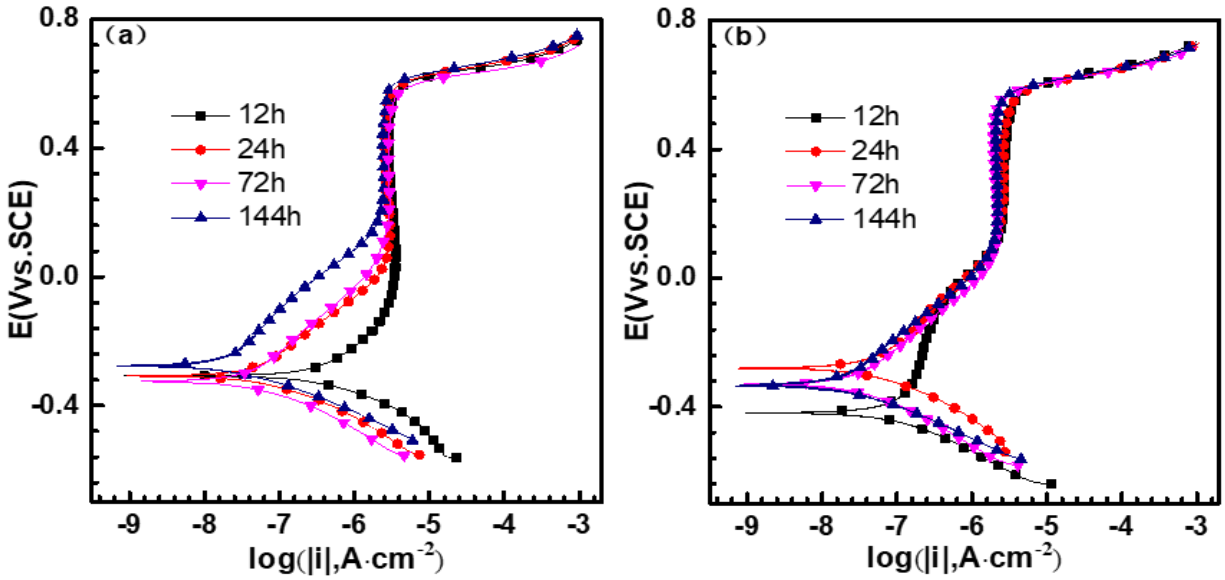

Figure 3. The polarisation curves of steel rebar passivation for 12 h, 24 h, 72 h and 144 h in SC and CE: (a) SC (b) CE

The polarisation curves of the rebar immersed for 7 days in SC and CE are shown in Fig. 3**Error! Reference source not found.**. The curves had obvious passivation characteristics, and the passivation interval decreased after immersion for 1 day. Table 2 shows the fitting results of the polarisation curves. With a prolonged immersion time, the polarisation curve shifts positively, the corrosion current density (I_{corr}) decreases. At the same immersion time, the I_{corr} of rebar in CE is less than that in SC, meaning

that the passivation film formed in CE is steadier and has stronger corrosion resistance than the film formed in SC. After 24 hours of immersion, the I_{corr} of both steel rebars was less than 0.1 μA/cm^2, indicating that the steel rebar can form a protective passivation film after being immersed for 1 day in SC and CE, which is in good agreement with the findings of Liu et al. [22].

Table 2. Fitting results of the polarisation curves in SC and CE.

Time (h)	I_{corr} (μA/cm^2)		E_{corr} (V_{SCE})	
	SC	CE	SC	CE
12	3.16×10^{-1}	9.17×10^{-2}	-0.308	-0.422
24	5.49×10^{-2}	4.82×10^{-2}	-0.308	-0.279
72	4.25×10^{-2}	4.05×10^{-2}	-0.326	-0.329
144	2.56×10^{-2}	2.23×10^{-2}	-0.276	-0.333

3.3 EIS measurements

EIS can analyse the structural characteristics of passivation films on steel surfaces [23]. Fig. 4 and 5 show the EIS of steel rebars immersed in SC and CE for different times. The Nyquist diagram shows the capacitive resistance characteristics, and after 7 days of immersion, the radius of capacitive arc resistance at low frequency increases, which indicates that the corrosion resistance of steel rebar is obviously improved [24, 25].

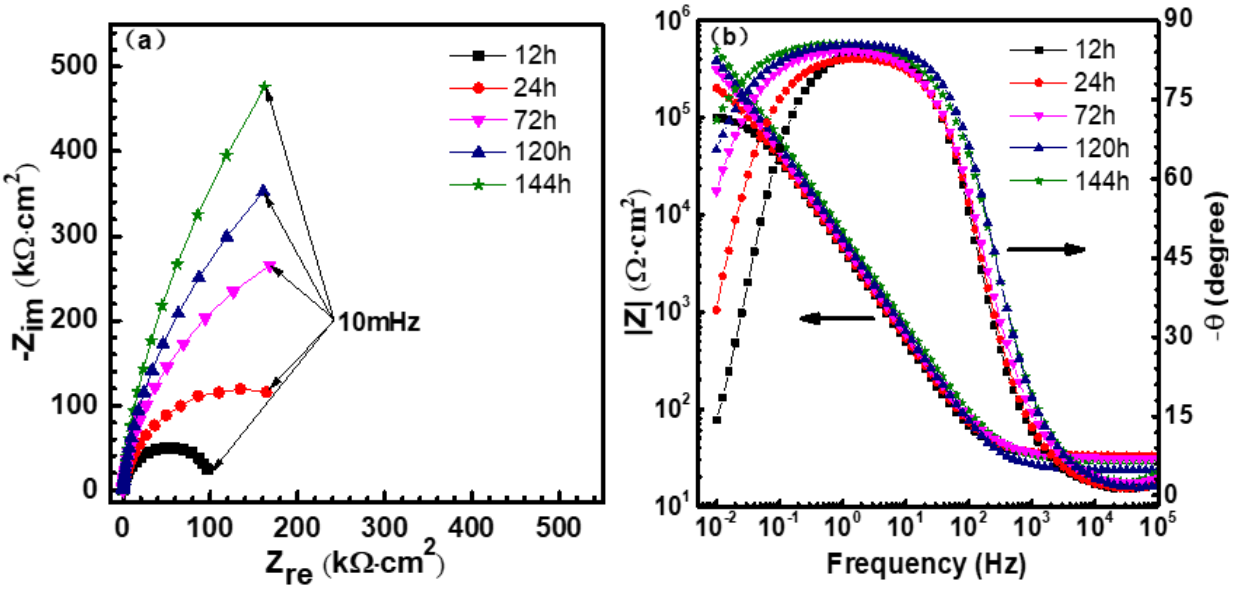

Figure 4. EIS of steel rebars immersed in SC for 12 h, 24 h, 72 h, 120 h and 144 h: (a) Nyquist plots and (b) Bode plots

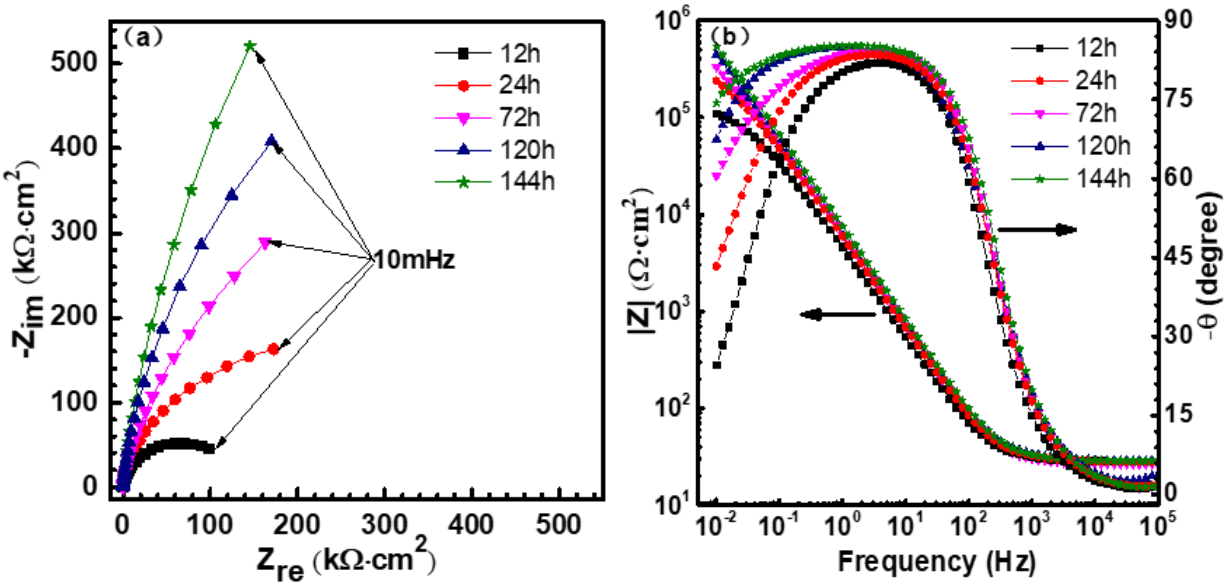

Figure 5. EIS of steel rebars immersed in CE for 12 h, 24 h, 72 h, 120 h and 144 h: (a) Nyquist plots and (b) Bode plots

In the extremely low frequency region of the Bode diagram, the polarisation impedance is shown of the impedance modulus response electrode [26]. In the figure, the polarisation impedance increases with immersion time, indicating that the stability of the passive film increases. At the same time, the phase angle in the frequency domain moves upwards as the peak becomes wider. The phase angle width of 144 hours is approximately twice that of 12 hours, which indicates that there are two time constants.

EIS data were analysed with an equivalent circuit diagram [27], as shown in Fig. 6. In this circuit, R_s represents the solution resistance, Q_{dl} represents the electric double layer capacitance, R_{ct} is the charge transfer resistance of the steel/solution interface, R_f is the resistance of the passive film, and Q_f represents the passivation film double layer capacitor.

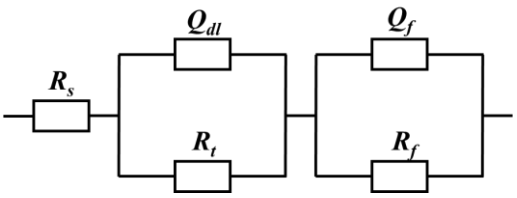

Figure 6. Equivalent circuit of EIS used in this experiment

The electrochemical capacitance of Q is usually calculated by the following formula [28]:

$$C_f = (QR)^{1/n}/R$$

where Q is CPE, n is the index of Q, and R is the passive film resistance.

The curves of R_{ct} and R_f over immersion time are shown in Fig. 7 by EIS fitting data. The R_{ct} and R_f of steel rebars increased after 7 days immersion in SC and CE, indicating that the stability of the passive film was improved. At the same immersion time, the R_{ct} and R_f of passivation film in CE are

larger than those in SC, which indicates that the passivation film formed by the steel bar in CE is more protective.

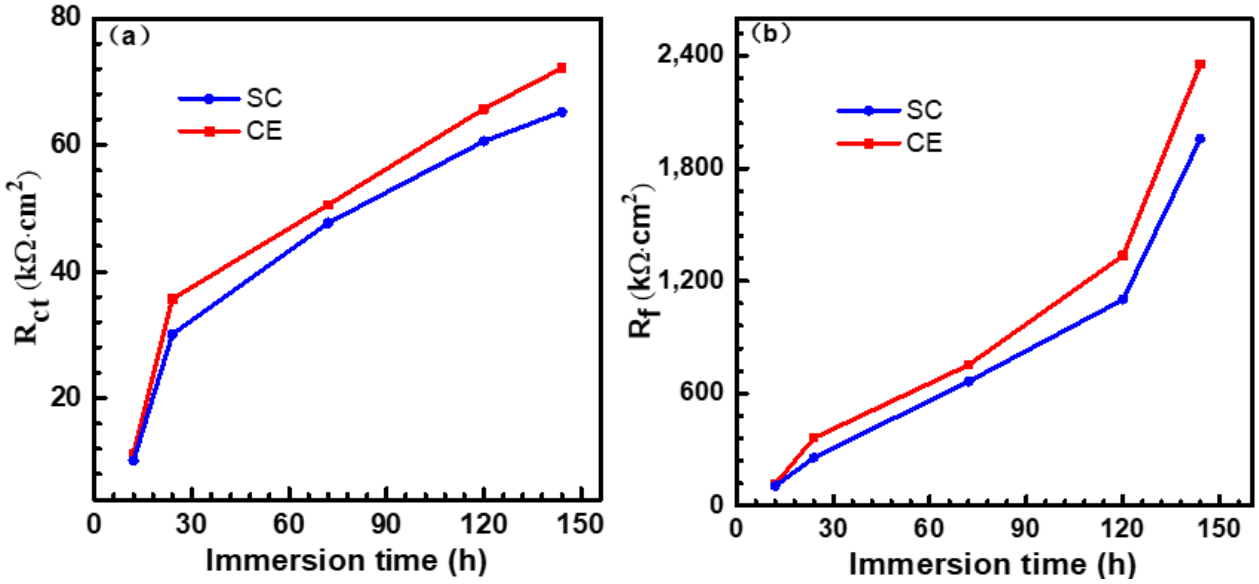

Figure 7. Variation of (a) R_{ct} and (b) R_f of steel rebars in SC and CE over the immersion time

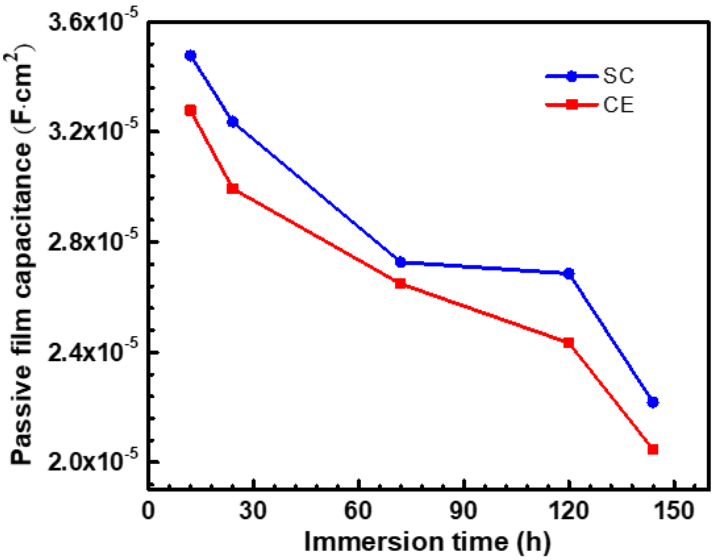

Figure 8. Variation of C_f with the passivation time

Fig. 8 shows the change curve of passive film capacitance C_f over immersion time. C_f decreases with the prolongation of passivation time, which is attributed to the thickness of the passive film increasing gradually. After 7 days of immersion, the C_f corresponding to CE is lower than that of SC, which indicates that the passive film formed in CE is thicker.

3.4 Capacitance results

The passive film has semiconductor characteristics, and studying the semiconductor properties of passive film is helpful for understanding the corrosion resistance mechanism [29]. According to the semiconductors type, all semiconductors with donor impurities or more donors than acceptors are n-type semiconductors, and vice versa for a p-type. The relationship between space charge capacitance and the potential of n-type and p-type can be calculated as follows [30-32]:

$$\frac{1}{C^2}=\frac{2}{\varepsilon\varepsilon_0 eN_D}\left[E-E_{fb}-\frac{kT}{e}\right] \quad (1)$$

$$\frac{1}{C^2}=-\frac{2}{\varepsilon\varepsilon_0 eN_A}\left[E-E_{fb}-\frac{kT}{e}\right] \quad (2)$$

where ε is the relative dielectric constant of the passive film (ε =12) [21, 33]; e is the electron charge; ε_0 is the vacuum dielectric constant (8.85×10^{-12} F/m); K is the Boltzmann constant (K=1.38×10^{-23} J/K); T is the absolute temperature; N_D is the electron donor concentration; and N_A is the electron acceptor concentration. The Mott-Schottky curve is obtained by plotting 1/C^2 and the potential E. The slope of the curve of n-type is positive and that of p-type is negative.

Fig. 9 shows the M-S curve of the steel bars immersed in SC and CE for different times. From the figure, the potential range of the n-type semiconductor characteristic is -1.0 to 0.5 V_{SCE}, and the slope of the curve is positive.

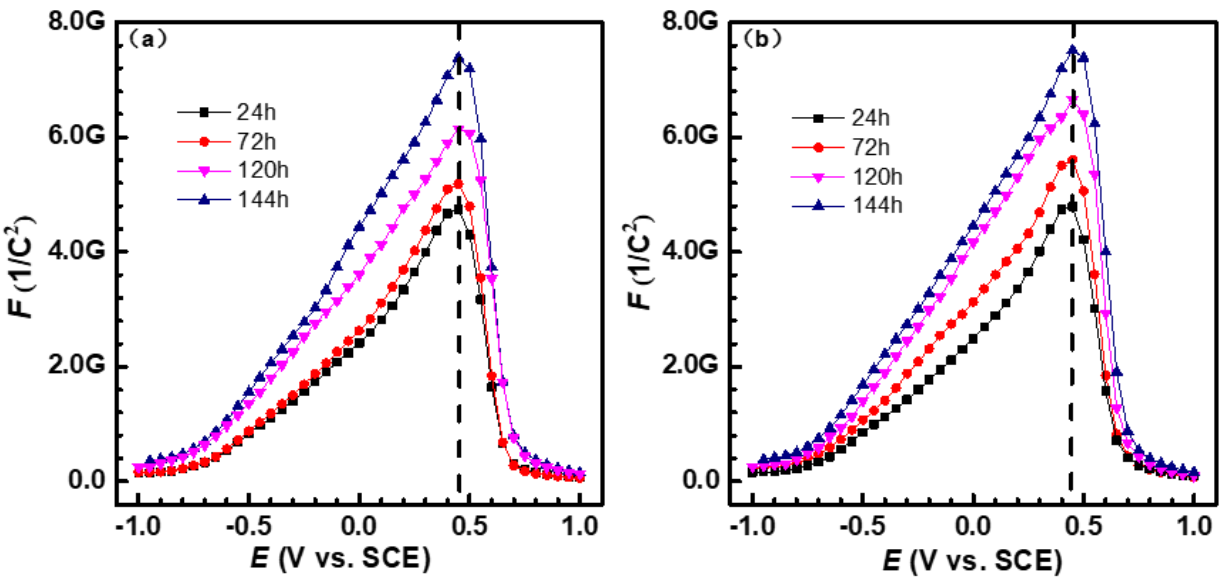

Figure 9. Mott-Schottky curves of steel rebars in SC and CE (a) SC and (b) CE

From 24 hours to 144 hours, the slope of the n-type semiconductor curve increases, and the space charge capacitance increases. Based on the point defect model [34], the donor carrier concentration N_D can be used to represent the number of point defects. The larger the donor concentration, the worse the density of the passive film is, which increases susceptibility to damage. Table 3 shows the donor carrier

concentrations N_D and E_{fb}. The carrier concentration of the passive film decreases from 24 hours to 144 hours, which indicates that the number of defects decreases and the density increases. At the same time, the carrier concentration of the steel passivation film in CE is lower than that in SC, which indicates that the passivation film formed in CE has better stability, compactness and corrosion resistance, which correlates with the results of impedance spectroscopy.

Table 3. Fitting parameters of the Mott-Schottky curve of steel rebars in SC and CE

Time	$N_D/10^{21}cm^{-3}$		E_{fb}/V	
(h)	SC	CE	SC	CE
24	3.417	3.370	-0.757	-0.751
72	3.062	2.803	-0.733	-0.783
120	2.489	2.169	-0.885	-0.799
144	2.057	1.971	-0.847	-0.863

3.5 XPS

The passive film of steel rebars immersed for 7 days in SC and CE was analysed by XPS. Table 4 shows the peaks of the binding energies of the main compounds of Fe, Cr, O and Ca in the passivation film.

Table 4. Peak value of the binding energy for the main compounds in the passivation film

Element	Peak	Species/binding energy (eV)		
Fe	$2p_{3/2}$	Fe(met)	FeO	FeOOH
		707.7	709.4	711.8
Cr	$2p_{3/2}$	$Cr(OH)_3$	CrO_3	/
		577.1	578.2	/
O	1s	O^{2-}	OH^-	H_2O
		530.2	531.8	533.0
Ca	$2p_{3/2}$	$CaCO_3$	/	/
		346.8	/	/

Fig. 10 shows the XPS spectra. The energy spectrum of Fe has three component peaks, Fe(met), FeO and FeOOH, in which the intensity of FeOOH is highest. The energy spectrum of Cr includes CrO_3 and $Cr(OH)_3$. The corresponding peaks of the two substances are relatively low, indicating that their contents are relatively low. The Ca element has two peaks corresponding to $CaCO_3$, and the energy spectrum of the O element has three component peaks: O^{2-}, OH^- and H_2O, in which the OH^- peak is significantly higher than O^{2-} and H_2O.

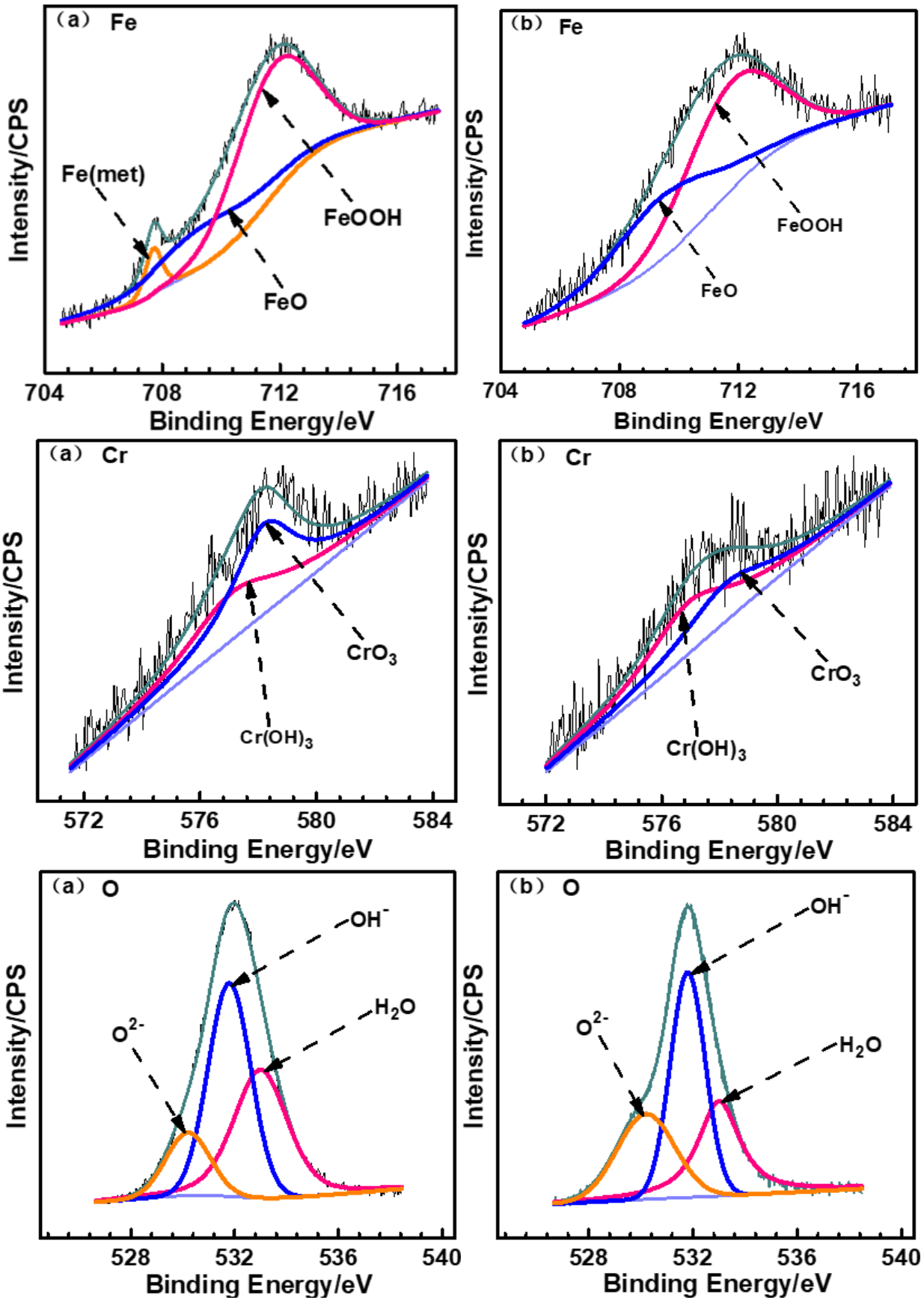
(a) Fe
Fe(met)
FeOOH
FeO
Intensity/CPS
704
708
712
716
Binding Energy/eV
(b) Fe
FeOOH
FeO
Intensity/CPS
704
708
712
716
Binding Energy/eV
(a) Cr
CrO3
Cr(OH)3
Intensity/CPS
572
576
580
584
Binding Energy/eV
(b) Cr
CrO3
Cr(OH)3
Intensity/CPS
572
576
580
584
Binding Energy/eV
(a) O
OH-
H2O
O2-
Intensity/CPS
528
532
536
540
Binding Energy/eV
(b) O
OH-
H2O
O2-
Intensity/CPS
528
532
536
540
Binding Energy/eV

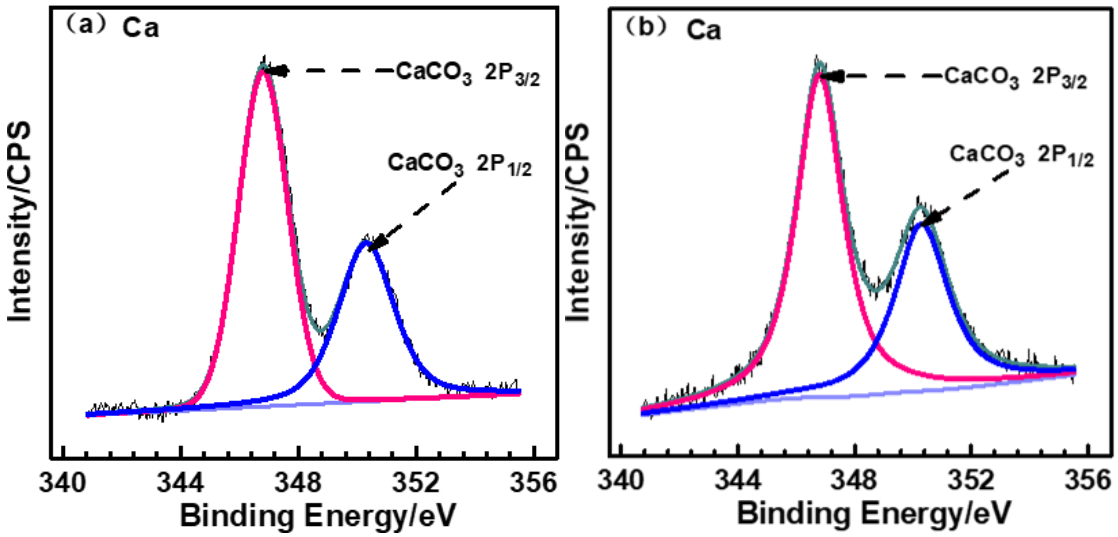

Figure 10. XPS spectra of steel rebars immersed in SC and CE for 7 days (a) SC (b) CE

According to the peak area corresponding to the substance in the passivation film binding energy spectrum, the percentage ratio of the corresponding substances of the four elements (Fe, Cr, O, Ca) shown in Fig. 11a was calculated. The passivation film formed in SC and CE has the same composition, including oxides of Fe and Cr, and $CaCO_3$. The passive film formed in SC can detect Fe(met), which indicates that the thickness of the passive film is approximately several nanometres [35]. During the passivation of the steel bar, the Cr element participates in the formation of the passivation film to form $Cr(OH)_3$ and CrO_3. Cr^{3+} is conducive to the self-repair and stability of the passive film [36]. In CE contains high Cr^{3+} content, indicating good stability. Comparing the $CaCO_3$ content in SC and CE, the passive film formed in SC contains more $CaCO_3$. The $CaCO_3$ precipitate can be deposited in the pores and microcracks, inhibiting the formation of the passive film, reducing its compactness and increasing the defect concentration. Fig. 11b shows that compared with SC, CE contains less bound water and more OH^-, which corresponds to a large amount of FeOOH and $Cr(OH)_3$ in the passive film.

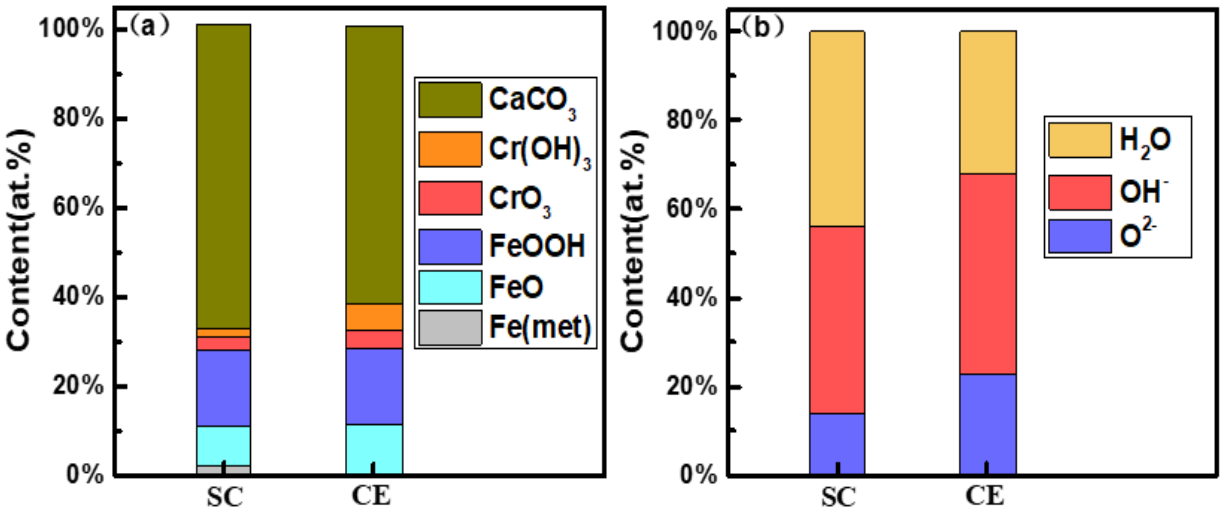

Figure 11. Percentage content ratio of four elements in the passive film

3.6 CPP measurements

CPP were carried out to compare the pitting corrosion resistance between the passivated and unpassivated steel bars. The pitting potential (E_{pit}) is defined as the potential at which the current density increases sharply, and the repassivation potential (E_{rep}) is defined as the potential at which the anodisation and the anti-polarisation curve intersect [22]. The results show that when the potential E_{rep} is higher than E_{pit}, pitting will not occur; when E_{rep} is lower than E_{pit}, a lag loop appears in the curve, and pitting will occur [37, 38].

Fig. 12 shows the CPP curves of steel rebar passivated for 7 days immersed in SC and CE with different Cl^- concentration. When the Cl^- concentration is 1.8% (Fig. 12a), the shape of the two potentiodynamic polarisation curves (CPP) is similar, and there is no hysteresis loop. Moser et al. [39] indicated that the passive film structure is stable in this Cl^- concentration. When the Cl^- concentration increased to 2.0% (Fig. 12b), the shape of the SC curve obviously changed. At the same potential, the current density of the return sweep was higher than that of the forward sweep, the potential E_{rep} was lower than that of E_{pit}, and the passive film was pitted. Saremi et al. [40] confirmed that the formation of hysteresis loops indicates the development of corrosion pits on the surface of steel bars. Compared with the SC curve, the CE curve has no hysteresis loop, E_{rep} is still higher than E_{pit}; this indicates that the passive film formed in CE is more stable, the pitting corrosion resistance is better and the critical Cl^- concentration is higher. As the Cl^- concentration increased to 2.2% (Fig. 12c), hysteresis loops appeared in the CPP curve sweeping, showing obvious pitting behaviour. In summary, the critical Cl^- concentration of passive film formed in CE is higher than SC,and this result is consistent with the research of Liu et al. [18], who found that the passive film formed in CE has stronger pitting resistance.

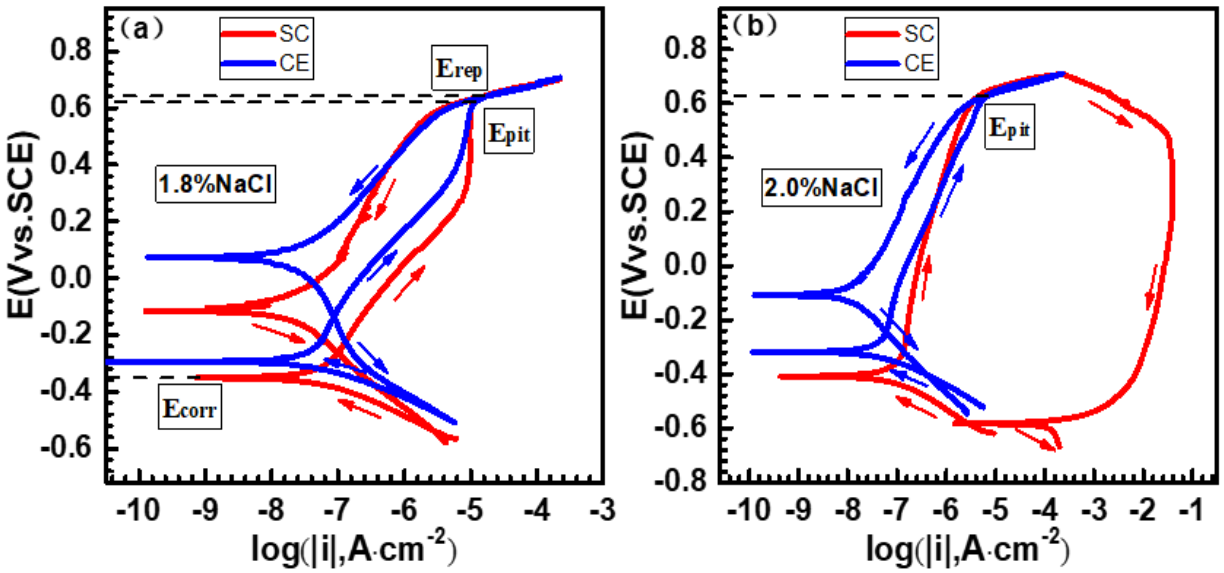

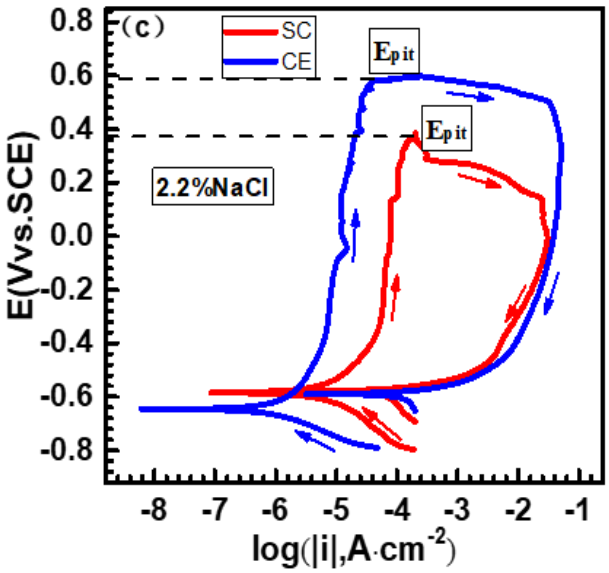

Figure 12. CPP curves of steel bar passivated for 7 days in SC and CE with different Cl^- concentrations

Fig. 13 shows the CPP curves of unpassivated steel rebars immersed in SC and CE with different Cl^- concentration. When the Cl^- concentration is 0.3%, no pitting corrosion occurs in SC and CE. When the Cl^- concentration is 0.5%, the SC curve maintained its original shape without pitting corrosion. The hysteresis loops of CE curves appear obviously, which is different from the curve (Fig. 13b) of steel rebars passivated for 7 days in SC and CE. This shows that the unpassivated steel bar samples have better Cl^- pitting resistance and higher critical Cl^- concentration in SC. As the Cl^- concentration increased to 0.7%, both showed significant pitting behaviour.

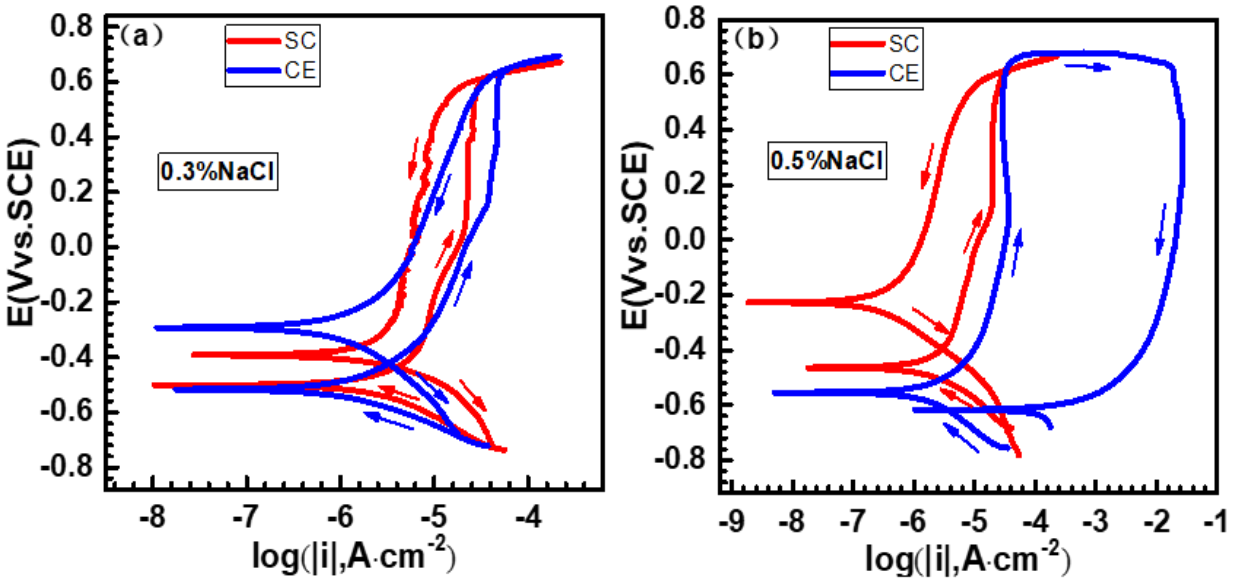

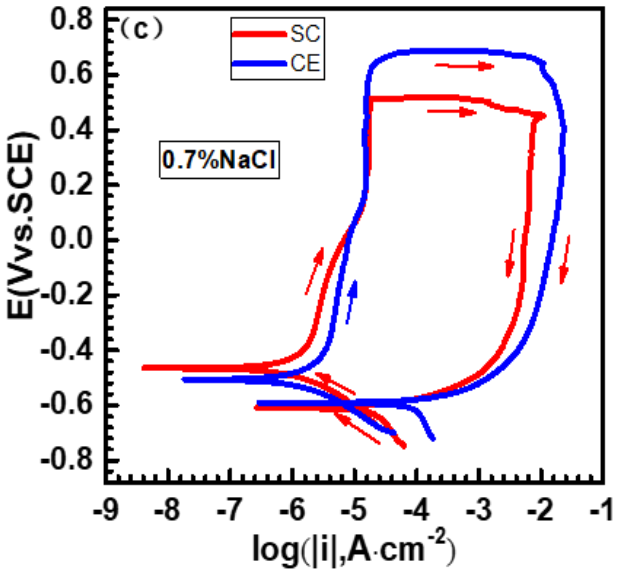

Figure 13. CPP curves of unpassivated steel bar immersed in SC and CE with different Cl^- concentrations

According to the CPP curves of the steel rebars without passivation and with passivation for 7 days, the results show that the unpassivated steel rebars have higher critical Cl^- concentrations in SC than in CE. Shi et al. [15] indicated that there are many kinds of ions in CE, including Na^+, K^+, Al^{3+} and SO_4^{2-}; these ions are easy to adsorb on the surface of steel rebars, leading to a decrease in the critical Cl^- concentration of the steel rebars. The critical Cl^- concentration of a passivated steel bar in CE is higher, and the critical Cl^- concentration of a passivated steel bar is approximately 4 times that of an unpassivated steel bar, which indicates that passive film can improve the pitting corrosion resistance of a steel bar.

4. CONCLUSION

1) At the beginning of the immersion, the formation rate of the passive film is relatively fast. As the immersion time increases, the OCP of low alloy steel rebars is positively shifted in SC and CE. After immersion for 24 hours, the open circuit potential remains stable.

2) With the same passivation time, the R_f and *Rct* values of the passivation film in CE are larger than those in SC, while the capacitance C_f and I_{corr} of the passivation film are lower, which indicates that the passive film formed in CE is thicker and has better stability than the film formed in SC. The passive film formed in SC and CE has n-type semiconductor characteristics. In CE, the donor carrier concentration of the passivation film is low, the number of point defects is small, and the passivation film formed is compact.

3) The passivation film formed in SC and CE has the same composition but in different ratios. Cr oxides are present in the passivation film, which indicates that Cr participates in the formation of the passive film.

4) The bare steel has a higher critical Cl^- in SC; however, after 7 days of passivation, the critical Cl^- of steel is higher in CE than in SC. The critical Cl^- concentration of the passivated steel bar is approximately 4 times higher than that of the unpassivated steel bar, which indicates that the passive film can significantly improve the pitting resistance.

ACKNOWLEDGEMENTS
The authors gratefully appreciate the financial support provided by the National Key R&D Program of China (2016YFE0203600) and the National Environmental Corrosion Platform (NECP).

References

1. J.J. Shi, D.Q. Wang, J. Ming and W. Sun, *J. Mater. Civ. Eng.*, 30 (2018) 04018042.
2. G.Y. Li, L.M. Ma, Z.Q. Zhang, J.H. Feng and J.Z. Li, *Iron Steel*, 41 (2006) 53.
3. M. Liu, X.Q. Cheng, X.G. Li, J. Zhu and H.X. Liu, *Constr. Build. Mater.*, 93 (2015) 884.
4. N. Mohamed, M. Boulfiza and R. Evitts, *J. Mater. Eng. Perform*, 22 (2013) 787.
5. D. Addari, B. Elsener and A. Rossi, *Electrochim. Acta*, 53 (2008) 8078.
6. P. Ghods, O.B. Isgor, F. Bensebaa and D. Kingston, *Corros. Sci.*, 58 (2012) 159.
7. Y. Zhang, A. Poursaee, *J. Mater. Civ. Eng.,* 27 (2014) 04014234.
8. Y.T. Tan, S.L. Wijesinghe and D.J. Blackwood, *Corros. Sci.*, 88 (2014) 152.
9. J.J. Shi, J. Ming and W. Sun, *Constr. Build. Mater.*, 155 (2017) 992.
10. H.B. Gunay, P. Ghods, O.B. Isgor, G.J.C. Carpenter and X.H. Wu, *Appl. Surf. Sci.*, 274 (2013) 195.
11. E. Volpi, A. Olietti, M. Stefanoni and S.P. Trasatti, *J. Electroanal. Chem.*, 736 (2015) 38.
12. C.Q. Ye, R.G. Hu, S.G. Dong, X.J. Zhang, R.Q. Hou, R.G. Du, C.G. Lin and J.S.Pan, *J. Electroanal. Chem.*, 688 (2013) 275.
13. M. Sánchez, J. Gregori, C. Alonso, J.J.G. Jareño, H. Takenouti and F. Vicente, *Electrochim. Acta*, 52 (2007) 7634.
14. J.J. Shi, W. Sun, J.J. Jiang and Y.M. Zhang, *Constr. Build. Mater.*, 111 (2016) 805.
15. J.J. Shi, J. Ming and W. Sun, *Corros. Sci.*, 736 (2015) 38.
16. L.H. Jiang, G.H. Huang, J.X. Xu, Y.R. Zhu and L.L. Mo, *Constr. Build. Mater.*, 30 (2012) 516.
17. Y. Peng, L. Liu, S.L. Wang, Y.H. Lin, Y.R. Sun and R.C. Xia, *J. Pet. Sci. Eng.*, 167 (2018) 949.
18. R. Liu, L.H. Jiang, J.X. Xu, C.S. Xiong and Z.J. Song, *Constr. Build. Mater.*, 167 (2018) 949.
19. S.M.A. Haleem, E.E.A. Aal, S.A. Wanees and A. Diab, *Corros. Sci.*, 52 (2010) 3875.
20. D. Song, J.J. Jiang and W. Sun, *Mater. Sci.*, 32 (2017) 1453.
21. M. Liu, X.Q. Cheng, X.G. Li, Y. Pan and J. Li, *Appl. Surf. Sci.*, 389 (2016) 1182.
22. M. Liu, X.Q. Cheng, G.C. Zhao, X.G. Li and Y. Pan, *Surf. Interface Anal.*, 48 (2016) 981.
23. W. Wu, W.K. Hao, Z.Y. Liu, X.G. Li, C.W. Du and W.J. Liao, *J. Mater. Eng. Perform.*, 24 (2015) 4636.
24. H. Luo, H.Z. Su, C.F. Dong, K. Xiao, and X.G. Li, *Constr. Build. Mater.*, 96 (2015) 502.
25. R.D. Moser, P.M. Singh, L.F. Kahn and K.E. Kurtis, *Corros. Sci.*, 57 (2012) 241.
26. H. Hasannejad, T. Shahrabi, A.S. Rouhaghdam and M. Aliofkhazraei, *J. Mater. Sci. Technol.*, 24 (2008) 715.
27. G.D. Eyu, G. Will, W. Dekkers and J.M. Leod, *Mater*, 9 (2016) 748.
28. H. Luo, C.F. Dong, X.G. Li and K. Xiao, *Electrochim. Acta*, 64 (2012) 211.
29. R.J. Jiang, Y.W. Wang, X. Wen, C.F. Chen and J.M. Zhao, *Appl. Surf. Sci.*, 412 (2017) 214.
30. J. Williamson, O.B. Isgor, *Corros. Sci.*, 106 (2016) 82.
31. Y.J. Zhang, A. Poursaee, *Anti- Corros. Methods Mater.*, 62 (2015) 363.

32. A. Xu, C.F. Dong, X. Wei, F.X. Mao, X.G. Li and D.D. Macdonald, *Electrochem. Commun.*, 68 (2016) 62.
33. G. Goodlet, S. Faty, P.P. Freitas, A.M.P. Simões, M.G.S. Ferreira and M.D.C. Belo, *Corros. Sci.*, 46 (2004) 1479.
34. D.D. Macdonald, *J. Electrochem. Soc.*, 139 (1992) 3434.
35. L. Freire, M.A. Catarino, M.I. Godinho, M.J. Ferreira M.G.S. Ferreira, A.M.P. Simões and M.F. Montemor, *Cem. Concr. Compos.*, 34 (2012) 1075.
36. M.G. Faichuk, S. Ramamurthy and W.M. Lau, *Corros. Sci.*, 53 (2011) 1383.
37. D.S. Gopi, M. Sayed, M. Surendiran, D.M.A. Sakila and L. Kavitha, *Surf. Interface Anal.*, 47 (2015) 5.
38. D. Gopi, M. Sherif, D.M.A. Sakila and L. Kavitha, *Surf. Interface Anal.*, 47 (2015) 618.
39. R.D. Moser, P.M. Singh, L.F. Kahn and K.E. Kurtis, *Corros. Sci.*, 57 (2012) 241.
40. M. Saremi, E. Mahallati, *Cem. Concr. Res.*, 32 (2002) 1915.